LAPPEENRANTA UNIVERSITY OF TECHNOLOGY
LUT School of Energy Systems
LUT Mechanical Engineering
BK10A0401 Kandidaatintyö ja seminaari

THE EFFECT OF FOCAL POINT PARAMETERS IN FIBER LASER WELDING OF STRUCTURAL STEEL

POLTTOPISTEEN PARAMETRIEN VAIKUTUS RAKENNETERÄKSEN KUITULASERHITSAUKSESSA

Joni Reijonen 13.5.2015
Examiner: Professor Antti Salminen

TABLE OF CONTENTS

SYMBOLS AND ABBREVITATIONS

LIST OF SYMBOLS AND ABBREVITATIONS

A_s	Surface area exposed to laser beam [mm^2]
D	Focal point diameter [mm]
D_r	Raw beam diameter [mm]
D_s	Beam diameter at surface [mm]
E_l	Line energy [J/m]
E_{sp}	Specific point energy [J]
f	Focal length [mm]
f_c	Collimation length [mm]
L_{fpp}	Distance between focal point and material surface [mm]
P	Laser power [W]
q_p	Power density [W/m^2]
v	Welding speed [m/s]
τ_i	Interaction time [s]
Θ	Divergence angle [mrad]

BPP	Beam parameter product
CEV	Carbon equivalent value
fpp	Focal point position
HAZ	Heat affected zone

1 INTRODUCTION

Development of multi-kilowatt fiber lasers in the early 2000's provided the welding industry an appealing alternative over CO_2-laser. Shorter wavelength of 1070 nm means better absorption on steels and enables beam delivery in an optical fiber for more flexibility. Good quality of the beam even at multi-kilowatt power levels together with small focal point diameter enables high enough power density for keyhole formation (Quintino et al., 2007, p. 1231–1237.) In keyhole welding, a deeply penetrating vapor cavity surrounded by molten material is produced to the work piece, resulting in a deep and narrow weld with good quality. This means that thick sections can be welded in a single-pass to compete with multi-pass arc welding in the means of productivity (Salminen, Lappalainen & Purtonen, 2013, p. 331–332.) Because of the considerably lower heat input of laser welding, distortions caused to the product are minimal and the heat affected zone is much narrower, making it a viable process in the welding industry.

Producing a good quality laser weld requires controlling the various laser beam and process parameters. Same depth of penetration can be achieved with different combinations of laser power, welding speed and focal point diameter (Suder & Williams, 2014, p. 223–229). However even if the penetration depth is the same, other properties of the formed welds vary depending on the parameter combination used. In this thesis the effect of focal point parameters in fiber laser welding of structural steel is studied. The goal is to establish relations between laser power, focal point diameter and focal point position with the resulting quality, weld-bead geometry and hardness of the welds.

In laser welding the gap tolerances for the joints are extremely demanding and these could be eased by increasing the focal point diameter and thus producing a wider weld. However if the focal point diameter is increased and welding speed kept the same, laser power has to be increased to achieve the same depth of penetration. Concurrently, with higher laser power the energy brought to the process is increased. How do these changes affect the resulting quality and properties of the weld?

The study is limited to structural steel, because it is the most used steel type in constructions that use several millimeters thick materials that are joined with welding, for example the shipbuilding industry. The material is also such that the assumed effects of the parameter variables should be distinguishable. Literature survey on recent scientific articles on the topic was done and a background was established. In addition, a set of welding experiments were done on structural shipbuilding steel AH36 having yield strength of 355 MPa to define how the variation of focal point parameters affects the resulting welds. Visual and macroscopic inspection was used to evaluate the quality and geometry of the welds produced. Hardness of the welded material was measured to evaluate the mechanical properties of the joint. All the inspections were done according to appropriate standards and the experimental methods are explained in detail in its own chapter.

2 LITERATURE REVIEW

In this chapter the principles of fiber laser keyhole welding are explained, along with typical phenomena in laser welding of structural steels. Parameters related to the focal point are introduced and the studies conducted by others on the effects of focal point parameters to the resulting weld properties are researched.

2.1 Laser

The word laser is an acronym for Light Amplification by Stimulated Emission of Radiation. Einstein (1916, p. 318–323) showed that electromagnetic radiation, i.e. light, consists of photons emitted by the light source either spontaneously or through stimulation. Furthermore he calculated that if an atom ready to emit a photon at some random time to a random direction (spontaneous emission) was passed by a stray photon, the atom would be stimulated by the stray photons presence and this would cause the atom to emit its photons. Considering lasers, the remarkable feature of this stimulated emission of radiation is that the photons emitted go exactly to the same direction as the original photon and have exactly the same frequency. This laid the foundation for amplifying light to generate a high intensity beam of light which is coherent, collimated and monochromatic and therefore has great focusability. (Einstein, 1917, p. 121–128.)

The theory for a laser was published by Schawlow and Townes (1958, p. 1940–1949) and based on this the first laser was made by Maiman (1960, p. 493–494), as he used light from a flash light to excite synthetic ruby in which the stimulated emission occurred and a laser beam was generated. All the lasers today work with the same principle. To generate a laser beam, some laser active medium is excited to a higher energy level by pumping light energy into it. This causes stimulated emission of radiation with same wavelength, which depends on the type of active medium used. The resulted radiation is then amplified in an optical cavity called resonator. This is done to achieve higher power beam by circulating the radiation through the medium multiple times by having two parallel reflectors at the ends of the resonator. At least one of the reflectors has to be partially transmissive so that the beam can get out and it can be used for materials processing. (Schawlow & Townes, 1958, p. 1940–1949.)

Every laser share the same principle, but the active medium and pump source can be different to achieve different wavelengths and more efficient pumping. The use of CO_2 gas as the active medium dominated the first decades of industrial lasers and still has a major role, although today various solid state lasers share the market. However the raw beam coming from the resonator isn't suitable for materials processing as it is. First the beam has to be transported to the working station and there collimated and focused to achieve smaller spot size at the work piece. When the power of the raw beam is focused on a small spot the resulted power density is high enough for welding applications. Deep penetration laser welding was first demonstrated by Brown and Banas (1971) with a CO_2-laser, when they achieved power density of around 1 MW/cm^2 which is high enough for excessive vaporization of steel to generate a keyhole.

2.1.1 Fiber laser

Fiber laser represents the new generation of solid state lasers in materials processing and it offers several benefits over other types of lasers. First fiber laser suited for materials processing was introduced in 2000 and it had output power of 100 W (Hill, 2002, p. 9). Today fiber lasers with multi-kilowatt output powers are available for materials processing, commercial systems having up to 100 kW powers. These multi-kilowatt systems are built by combining the output power of several single-mode lasers, each producing typically 400 or 800 watts. This way of increasing power means that the beam quality is only slightly decreased in the progress. When comparing different laser systems (CO_2, disk, Nd:YAG and fiber) fiber laser offers the lowest life-time costs, has the smallest footprint and a high wall plug efficiency of over 30 % (IPG Photonics, 2015; Katayama, 2013, p. 104; Quintino, et al., 2007, p. 1232; Ream, 2004, p. 4).

In a fiber laser the beam is generated in a silicon fiber that contains a core doped with rare earth, which is the lasing media. The core is stimulated with light from a diode laser which causes the active media to emit photons at a certain wavelength, depending on the rare earth used. The principle of generating laser beam in a fiber can be seen from figure 1. The laser system used in the experimental part of this work uses ytterbium as the lasing media, which emits photons at a wavelength of 1070 nm. Unlike the wavelength of CO_2-laser that is ten times higher, the light coming from a fiber laser can be transporter in an optical fiber to the processing head, increasing the flexibility of the workstation. The same laser source

can be used for different processes like cutting or welding by changing the processing head accordingly. The raw beam coming from the transport fiber is collimated and then focused by the optics contained inside a welding head to achieve small enough focal point diameter that can be used for keyhole welding.

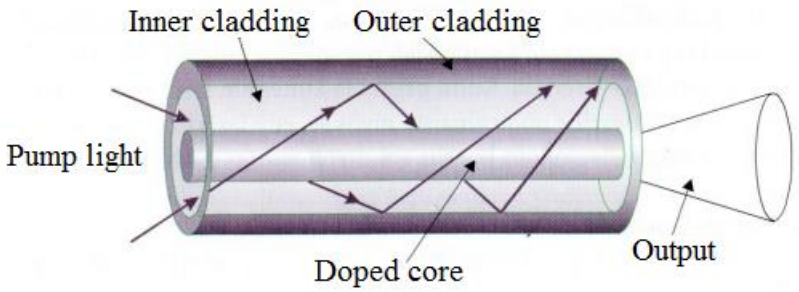

Figure 1. Laser beam generation in a fiber laser (modified: Kujanpää, Salminen & Vihinen, 2005, p. 68).

2.2 Laser beam-material interaction in fiber laser welding of structural steels

When the laser beam hits the surface of the material, part of the energy it contains is reflected away from the material and the rest is either absorbed or transmitted. In case of steels, the part that is transmitted is close to zero and it can be said that the energy is either reflected or absorbed. For laser materials processing high absorptivity is desirable as it increases the effectiveness of the process. As can be seen from figure 2, absorptivity with steels increase as the wavelength decreases. This is one of the main benefits of fiber laser over CO_2-laser which produces ten times higher wavelength. In the figure the 1070 nm wavelength of a fiber laser is situated at the same vertical line as Nd:YAG-laser.

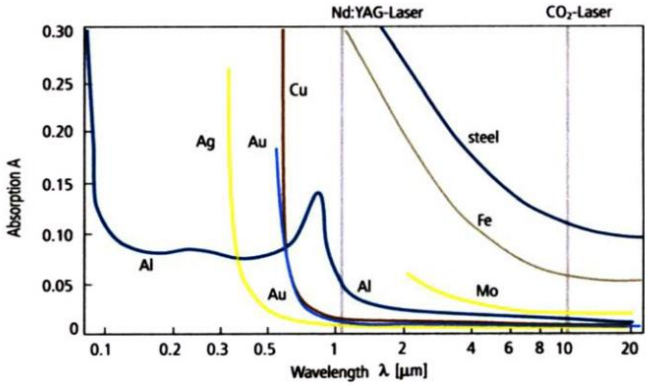

Figure 2. Absorption of light at different wavelengths on metallic materials in room temperature (Cleeman, 1987, p. 256).

As explained later, the absorption can be up to 90 % in keyhole welding because of the characteristics of the keyhole. The absorption percentages in figure 2 are valid at room temperature, i.e. for the first moments of the beam-material interaction, before the material starts to melt.

2.2.1 Weldability and typical imperfections

In general, structural steels are considered easy materials to be joined with welding. The weldability of a material can be evaluated by calculating the carbon equivalent value (CEV). This value is based on the chemical composition of the material and it can be used to evaluate the susceptibility to cold cracking and to the formation of martensite, which results in an increased hardness at the weld zone. This is undesirable, as it means that the mechanical properties of the joint may have reduced. According to International Institute of Welding materials with a CEV below 0.41 are considered to have good weldability and the values can be calculated as follows:

$$CEV = C + \frac{Mn}{6} + \frac{Cr+Mo+V}{5} + \frac{Cu+Ni}{15} \quad (1)$$

In equation 1, C is carbon, Mn is manganese, Cr is chromium, Mo is molybdenum, V is vanadium, Cu is copper and Ni is nickel, all in weight percentages. (International Institute of Welding, 1967.) AB AH36 structural steel was used in the experimental part of this thesis and it has a CEV of 0.248, calculated based on the values listed in table 1. However a low carbon equivalent value doesn't guarantee a sound weld, as there are other imperfections that can be produced. For laser welded joints, the limits for accepted imperfections for each quality level are stated in standard SFS-EN ISO 13919-1. Typical imperfections for butt welded joints can be seen from figure 3. All of these are caused by incorrect set of parameters or by misalignment of the work pieces or of the laser beam.

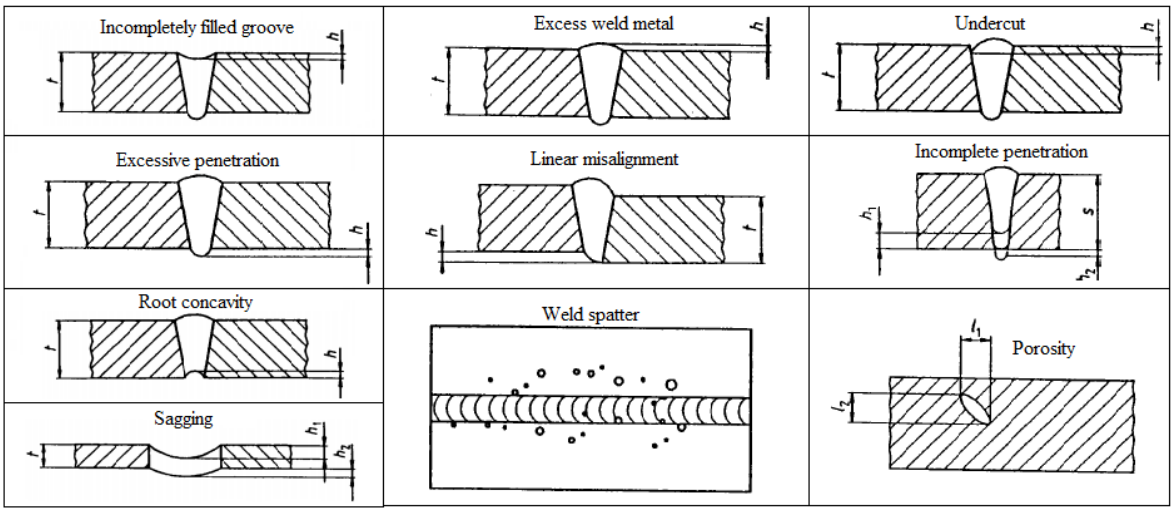

Figure 3. Imperfections seen on laser welded butt joints (modified: SFS-EN ISO 13919-1, 1996, p. 6–12).

2.3 Keyhole welding with fiber laser

Laser beam welding can be divided into two different categories, namely conduction-limited welding and keyhole welding, defined by the power density at the work piece surface. With steels a power density around 1 MW/cm^2 is considered the critical value between the two welding mechanisms. With power densities below this value the material is only melted and the heat conducts further to the material from the melt pool, which is similar to the arc welding processes. When the power density is increased the material starts to vaporize. The recoil pressure caused by the evaporating metal opens a vapor cavity to the molten material. This is called the keyhole and it is kept open by the vapor pressure as the forces caused by surface tension and hydrostatic pressure of the surrounding molten metal act to collapse the keyhole. (Ion, 2005, p. 395–397; Steen & Mazumder, 2010, p. 203–204.)

The laser beam is reflected multiple times from the walls of the keyhole and part of the energy of the beam is absorbed to the material every time. The phenomena is called Fresnel absorption. In full penetration laser welding this means that heat is brought to the joint along the whole thickness of the material and a narrow weld is produced with high melting efficiency. In keyhole welding the absorption of the beam can be over 90 % and the absorption increases as the depth of the keyhole increases. This is caused by the increased number of reflections of the beam inside the keyhole. (Kawahito et al., 2011, p. 1567.) The

Fresnel absorption is also higher at the bottom of the keyhole than close to the surface, meaning that at the bottom more metal is vaporized and the recoil pressure is higher which counters the increase in the hydrostatic pressure at the bottom, keeping the keyhole open all the way. (Xiangzhong et al., 2012, p. 7.) The process is illustrated in figure 3.

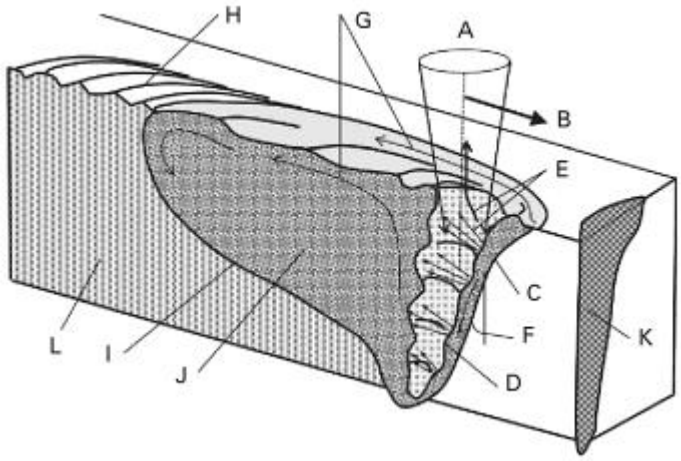

Figure 3. Weld bed formation in keyhole welding. A: Laser beam; B: Welding speed; C: Keyhole front; D: Humps; E: Vapor Jets; F: Keyhole front wall inclination; G: Melt flow; H: Chevron structure; I: Solidification front; J: Melt pool; K: Weld seam cross section; L: Solidified material (Katayama, 2013, p. 50).

Stability of the keyhole is required to produce a successful weld free of defects and with full penetration along the whole weld. Studies on dynamics of the keyhole, the surrounding melt pool and the vapor plume that is ejected have been of increased interest, as this could lead to an understanding of how the weld bed geometry and defects on the weld seam are formed.

Typically porosity is not a problem with laser keyhole welding, but sudden closures and re-openings of the keyhole causes gas traps inside the molten material, which is seen as porosity once the molten material solidifies. Keyhole collapses when the pressure caused by surface tension exceeds the recoil pressure of the vapor plume. This can be avoided by increasing laser power and thus increasing the evaporation rate of the material. Collapse of the keyhole also results in the loss of penetration depth. (Pastor, Zhao & Debroy, 2001, p. 275–281.)

It was shown by Dausinger and Weberpals (2007, p. 858–865) that welding speed is a crucial parameter for the keyhole behavior, as it changes the inclination angle between the laser beam and the keyhole front and also the inclination of the forming vapor plume. Increase in welding speed leads to an increase in the inclination angle so that the keyhole is more tilted from root backwards in relation to the incoming laser beam. Concurrently, this changes the direction of the ejecting vapor jet which blows up the molten material behind the keyhole and results in spatter formation. With lower welding speeds the ejection of the vapor plume is directed more perpendicular in relation to the material surface and the force of the vapor jet is suppressed by the increased molten material in the way of the vapor jet. (Dausinger & Weberpals, 2007, p. 858–865.)

Recently it was shown by Tenner et al. (2015, p. 32–41) that laser power also has an effect on the inclination angle of the vapor plume. Increasing laser power leads to an increase in the vapor plume inclination angle until the power reaches a threshold value of around 80 % of the power needed for full penetration. With laser power over this threshold value the geometry of the keyhole front wall changes. Before this the keyhole front wall could be considered a slope with a constant gradient that increased as the power increased. After exceeding the threshold power, the upper half of the keyhole front wall becomes more vertical and the slope starts from the lower half of the keyhole front wall. This moves the point of incidence deeper to the material and on the slope that has roughly the same gradient as earlier, thus the inclination angle is not increased further. Now that the point of incidence, where the evaporation rate is at highest, is deeper inside the material, the pressure of the vapor jet is increasingly suppressed by the molten material on its way. (Tenner et al., 2015, p. 32–41.)

2.4 Characteristics of focal point in laser welding

There are numerous parameters that have an effect on the quality of a laser welded joint and the goal of this work is to establish relations between the focal point characteristics and the resulting quality of the welds. For example, laser power and welding speed are crucial parameters that can be adjusted by the welding operator, but both affect the process through the characteristics of the focal point, which is the area where the laser beam is focused. When the diameter of the focal point is taken into consideration, power density and interaction time can be defined. These parameters can be used to estimate the geometry

and properties of the resulting welds and thus guide in the selection of the right welding speed and laser power. (Suder & Williams, 2014, p. 223–229.)

2.4.1 Focal point diameter

In laser processing the size of the area where the beam is focused is usually described as the diameter of the cross section of the beam at the focal point. Theoretical value for the focal point diameter of an ideal laser beam can be calculated as follows:

$$D = D_r \frac{f}{f_c} \tag{2}$$

In equation 2, D is focal point diameter, D_r is raw beam diameter, f is focal length and f_c is collimation length (Ion, 2005, p. 112). The diameter of the focal point is used to define the power density and interaction time of the laser beam, but in addition it has been show that it has an effect on the weld bead geometry. Increasing the focal point diameter leads to an increase in the weld width. (Suder & Williams, 2014, p. 228.) This is due to the increase in keyhole diameter and the diameter of the melt pool around it, resulting in a wider weld bead.

2.4.2 Power density

When the beam is focused, it will have a certain power density at the focal point which depends on the size of the focal point and of the laser power brought to that point. Power density can be calculated as follows:

$$q_p = \frac{4P}{\pi D^2} \tag{3}$$

In equation 3, q_p is average power density and P is laser power (Ion, 2005, 179). As can be seen from the equation, increasing laser power or decreasing the diameter of the focal point leads to an increase in power density. In previous studies it has been shown that penetration depth is proportional to the power density. In a study by Kawahito et al. (2007, p. 11–15) on the effects of power density in fiber laser welding of stainless steel it was concluded that increasing power density results in an increased penetration depth. However, it was shown by Katayama et al. (2010, p. 9–17) that with very high power densities and small

focal point diameters imperfections such as humping and undercut are produced. These defects are caused by the strong backward flow in the melt pool, induced by the increase in the ejecting vapor from the keyhole as power density increases (Katayama, Kawahito & Mizutani, 2010, p. 14).

2.4.3 Focal point position

In laser processing, focal point position is used to describe where the focal point is in relation to the surface of the material. When the laser beam is focused at the surface of the material, focal point position is zero. If the focus of the beam is raised above the material surface, the distance in between is considered as the positive axis and focal point position is given positive values of distance from the material surface. Focal point positions below the material surface receive negative values respectively. Focal point position tells where the narrowest beam is in relation to the material. Changing the position from zero results in a decrease of power density at the surface of the material.

One could reason that this would decrease the penetration depth, as it was shown earlier that decrease in power density leads to decreased penetration depth. However it was shown by Vänskä et al. (2013, p. 199-208) that this is not the case. In their experiments EN 1.4404 austenitic stainless steel samples of 8 mm in thickness were welded in a butt joint configuration. It was found that focal point positions up to 5 mm below the surface resulted in increased penetration depth, compared to focal point position at the surface. Focal point position of -5 mm meant that the beam diameter at the surface was more than doubled, yet the penetration depth was roughly the same as with focal point position at the surface. Lowering the focal point position even more resulted in a decrease in the penetration depth. (Vänskä et al., 2013, p. 202-203.)

As said before, the keyhole front wall inclination angle is a contributing factor to the behavior of the keyhole and the melt pool and understanding this has helped in the understanding of the mechanics behind formation of imperfections in the weld seam. In addition, it was shown by Vänskä et al. (2013, p. 206) that the keyhole inclination angle defines how the laser beam reflects inside the keyhole as it is more tilted backwards with increased inclination angle. This way the reflections are directed to the backside of the keyhole and not downwards deeper in to the material, reducing penetration depth. In addition to welding

speed, it was shown that focal point position also has an effect on the keyhole front wall inclination angle, as it increased with focal point positions deeper below the surface of the material. (Vänskä et al., 2013, p. 206.)

2.4.4 Interaction time

Welding speed and focal point diameter can be used to define interaction time, which defines the time how long a particular point, with the size of the beam diameter at the surface, is exposed to the laser beam. The maximum interaction time at the weld center line can be calculated as follows:

$$\tau_i = \frac{D_S}{v} \tag{4}$$

In equation 4, τ_i is interaction time, D_s is the diameter of the spot exposed to the laser beam and v is welding speed. It was proposed by Suder & Williams (2012, p. 032009-1–032009-10) that interaction time has an effect to the penetration depth and resulting width of the weld. With shorter interaction times the effect on penetration depth is greater and this can be explained with the utilization of energy brought to the process. The same amount of energy for a given material is always needed to initiate the keyhole and the rest is used for increasing penetration depth. With constant power density, shorter interaction time means that less energy is brought to the point. Now the energy needed to initiate the keyhole is still the same, so less energy is available for increasing the penetration depth. This means that as the energy brought to the process gets closer to the threshold value needed for initiating the keyhole, the slightest variations in the process parameters can lead to the collapse of the keyhole and thus drastically decrease the penetration depth. With longer interaction times the keyhole is more stable and the penetration depth is mainly controlled by power density. (Suder & Williams, 2012, p. 032009-2–032009-4.)

2.4.5 Line energy

In some studies, line energy is used as a measure for the energy brought to the process and then used for evaluating the weld hardness. Line energy is the relation of laser power and welding speed and can be calculated as follows:

$$E_l = \frac{P}{v} \quad (5)$$

In equation 5, E_l is the line energy. However, this study explores whether the suggested specific point energy is more accurate definition for the energy that is brought to the process, as it takes into consideration the area of the point, where the energy is brought. Increasing the area increases the energy that is brought.

2.4.6 Specific point energy

As described in chapter 2.4.4, interaction time affects the process through the energy that is brought to the process. The energy that is brought to a particular point at the material surface is described as specific point energy and it can be calculated as follows:

$$E_{sp} = q_p \tau_i A_s = P\tau_i \quad (6)$$

In equation 6, E_{sp} is specific point energy and A_s is the area of the point exposed to the laser beam. Note that this value is valid for constant interaction time across the point exposed to the laser beam and for beams with a uniform intensity distribution. Theoretically, this means a rectangular beam with top-hat intensity distribution, but the value is sufficiently accurate for top-hat beams with small focal point diameters, typical for laser welding. (Suder & Williams, 2012, p. 032009-4.)

As Suder & Williams (2012, p. 032009-5) studied the power density, interaction time and specific point energy they found out that even with constant interaction time and power density the penetration depth is not constant, but changes according to the focal point diameter used. That is why specific point energy needs to be considered, as it increases when increasing the focal point diameter, even with constant power density and interaction time, as can be seen from equation 6. It was found out that welds with constant specific point energies result in constant penetration depths, higher energies resulting in deeper penetrations. (Suder & Williams, 2012, p. 032009-5.)

3 EXPERIMENTAL METHODS

In this chapter the methods, materials and equipment used in the welding experiments are discussed in detail, so that the experiments can be re-produced. The experiments were conducted at room temperature and at normal atmospheric pressure.

3.1 Materials

Material used in the experiments was AB AH36 structural steel having yield strength of 355 MPa, with a typical chemical composition seen from table 1. This steel grade is widely used in the shipbuilding industry as a structural material. The plates used in the experiments were cut with a CO_2-laser using oxygen as the cutting gas. The surface areas of the joints were sandblasted before welding and wiped with acetone to remove any impurities.

Table 1. Chemical composition of AB AH36 steel used in the welding experiments, in weight percentages.

C	Si	Mn	P	S	Cr	Mo	Ni	Cu	Al	V
0.111	0.149	0.711	0.035	0.150	0.051	0.01	0.041	0.031	0.034	0.0083

3.2 Experimental setup

Two 8 mm thick, 300 mm long and 75 mm wide plates of AB AH36 steel were welded together in an I-butt joint configuration using IPG YLS-10000 continuous wave fiber laser. Two welds, each approximately 150 mm in length were done on each pair of plates. Precitec YW50 processing head was used with a focal length of 300 mm and collimation length of 150 mm to have a top-hat intensity distribution in the beam. Parameters of the laser beam for each processing fiber diameter can be seen from table 2. The shielding gas was brought to the process off-axial from a 45 degree angle. The excess metal vapor-cloud ejected from the keyhole was blown away with compressed air to ensure that the vapor doesn't interfere with the beam. The setup can be seen from figure 4.

Table 2. IPG YLS-10000 specification for each process fiber diameter.

Fiber diameter [µm]	Output power [kW]	Wavelength [nm]	Rayleigh length [mm]	Divergence angle [mrad]	BPP [mm*mrad]
200	10	1070	10.260	58.228	8.697
300	10	1070	11.600	59.753	10.354
600	10	1070	17.715	74.415	24.525

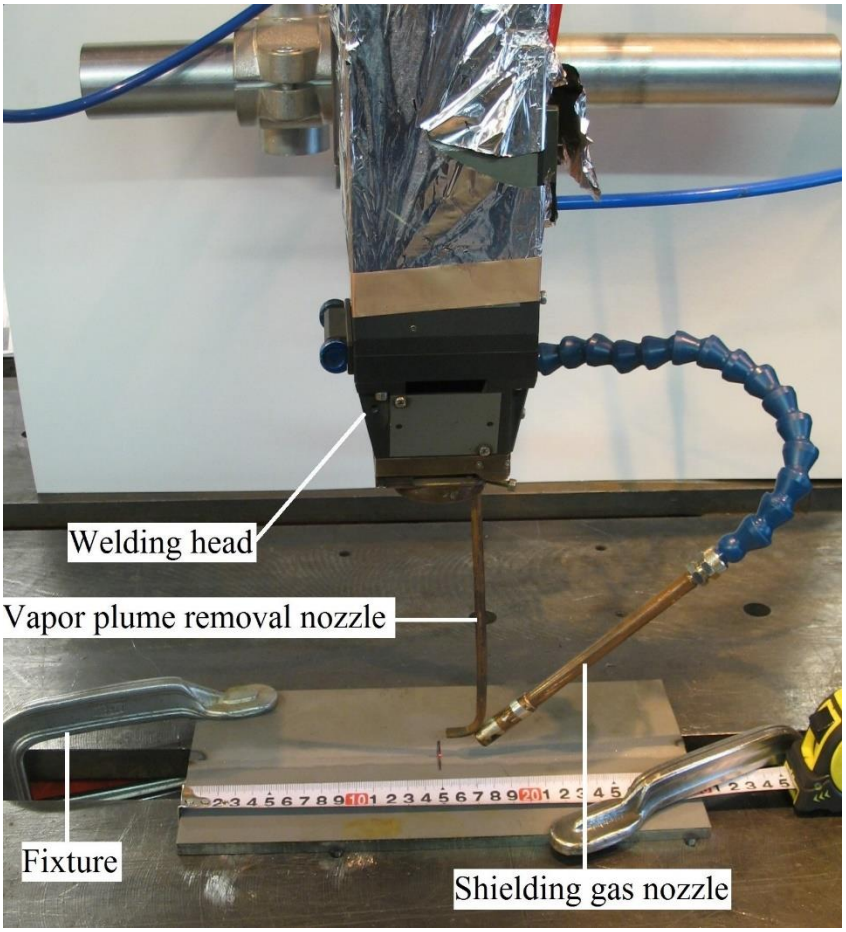

Figure 4. Experimental setup.

3.3 Experimental parameters

Welding speed was kept at a constant value of 1.25 m/min. The shielding gas used was argon and the flow rate was kept at 20 l/min in all experiments. Joint type was I-butt with zero air gap. Box-Behnken design was used in the selection of the parameter combinations. This means that the parameters are changed on three different planes at the same time to see the combined effect of all three variables. Parameters used in each experiment can be seen from table 3.

Table 3. Parameter combinations used in the experiments.

Exp.	Power [kW]	Focal point position [mm]	Fiber diameter [µm]	Focal point diameter [mm]	Surface point diameter [mm]	Power density [MW/cm^2]	Interaction time [ms]	Specific point energy [J]
1	7.0	-1.0	200	0.4	0.458	5.57	21.984	153.9
2	7.0	-1.0	300	0.6	0.660	2.48	31.680	221.8
3	7.0	-6.0	200	0.4	0.750	5.57	36.000	252.0
4	7.0	-3.0	300	0.6	0.779	2.48	37.392	261.7
5	7.0	-1.0	600	1.2	1.275	0.62	61.200	428.4
6	7.0	-6.0	600	1.2	1.647	0.62	79.056	553.4
7	6.0	-1.0	300	0.6	0.660	2.12	31.680	190.1
8	6.0	-3.0	200	0.4	0.575	4.77	27.600	165.6
9	6.0	-3.0	300	0.6	0.779	2.12	37.392	224.4
10	6.0	-3.0	600	1.2	1.424	0.53	68.352	410.1
11	5.0	-1.0	200	0.4	0.458	3.98	21.984	109.9
12	5.0	-1.0	600	1.2	1.275	0.44	61.200	306.0
13	5.0	-3.0	300	0.6	0.779	1.77	37.392	187.0
14	5.0	-6.0	600	1.2	1.647	0.44	79.056	395.3

For these process parameter combinations the corresponding focal point parameters were calculated based on equations 2, 3, 4 and 6. Note that these values are all calculated based on the theoretical value of the focal point diameter. The surface point diameters were calculated for each combination of transport fiber and focal point position used as follows:

$$D_s = D + L_{fpp} tan(\Theta) \quad (7)$$

In equation 7, D_s is surface point diameter, L_{fpp} is the distance between the material surface and focal point, i.e. focal point position and Θ is the divergence angle, which is different for each transport fiber that is used, as seen from table 2.

3.4 Qualitative analysis

The stability of the process was visually evaluated during welding and 100 % visual inspection was done for surface and root for each weld to identify defects visible to the eye.

The quality of the welds were evaluated based on standard SFS-EN ISO 13919-1, which defines three different quality levels depending on the type and severity of imperfections found on the welds. The three categories from best to worst are: B – stringent, C – intermediate and D – moderate. (SFS-EN ISO 13919-1, 1996, p. 1–16.)

3.4.1 Macroscopic inspection

After examination and photography of the surface and root of each weld, test specimens approximately 20 mm long and 30 mm wide were cut from the plates for macroscopic inspection of the weld cross-sections. The surface to be inspected was then polished and finally etched with Nital. This was all done according to standard SFS-EN ISO 17639 (2013).

3.4.2 Hardness evaluation

SFS-EN ISO 13919-1 doesn’t cover metallurgical aspects, but in addition hardness tests were done on part of the welds according to standard SFS-EN ISO 6507-1 (2006) to evaluate mechanical properties of the joints. The samples to be measured were selected so that possible differences in the hardness values would be distinguishable between the different parameters. Vickers hardness test with the weight of 5 kg was done to measure the hardness from the middle of the cross-sections. Depending on the width of the welds, 9 to 12 measuring points 0.4 mm apart were done along a vertical line to see the difference between base material, HAZ (heat affected zone), fusion line and the melt zone.

4 RESULTS AND ANALYSIS

The results of the welding experiments are presented in this chapter. Pictures of all of the welds can be seen in appendix I, which includes both the weld bead and root side for each weld, along with macrographs of the cross sections.

4.1 Weld quality

In the welds produced, lack of penetration was the only imperfection leading to an unacceptable weld, according to standard SFS-EN ISO 13919-1. In addition, other imperfections such as spatters and humps were produced, but these imperfections are only minor and inside the limitations set for B level weld quality in the standard. The results are plotted as specific point energy to power density for each weld, seen from figure 5. Acceptable welds are marked with squares and welds with incomplete penetration with triangles.

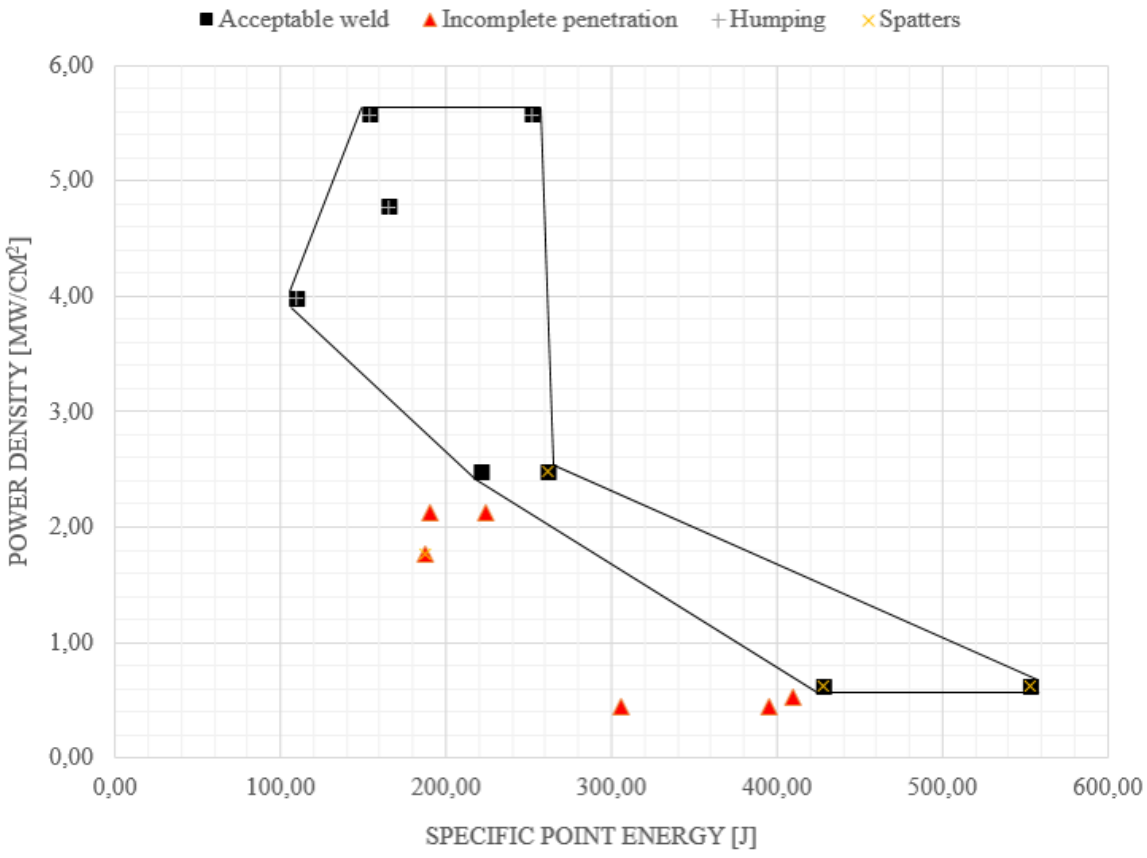

Figure 5. Quality window for 8 mm thick AH36 steel.

Figure 5 suggests that the penetration depth depends on power density and specific point energy. Full penetration welds are achieved either by having high power density or specific point energy. In Figure 6, this is studied in more detail and the indication is that a certain specific point energy is needed for a given power density to achieve full penetration. Macrograph a) in the figure shows a full penetration weld achieved with power density of 0.62 MW/cm^2 and specific point energy of 428.4 J. Macrographs b) and c) show welds with only partial penetration and incompletely filled groove, despite the increase in power density to 2.12 MW/cm^2, but at the same time the specific point energy was reduced to 224.4 J and 190.1 J respectively, which means that there was not enough energy brought to the process for complete penetration. Macrograph d) shows a weld with incomplete penetration, as the power density was reduced to 1.77 MW/cm^2. This shows that both the specific point energy and power density have to be sufficient for complete penetration. Reducing power density means that specific point energy has to be increased, or vice versa, to achieve the same penetration.

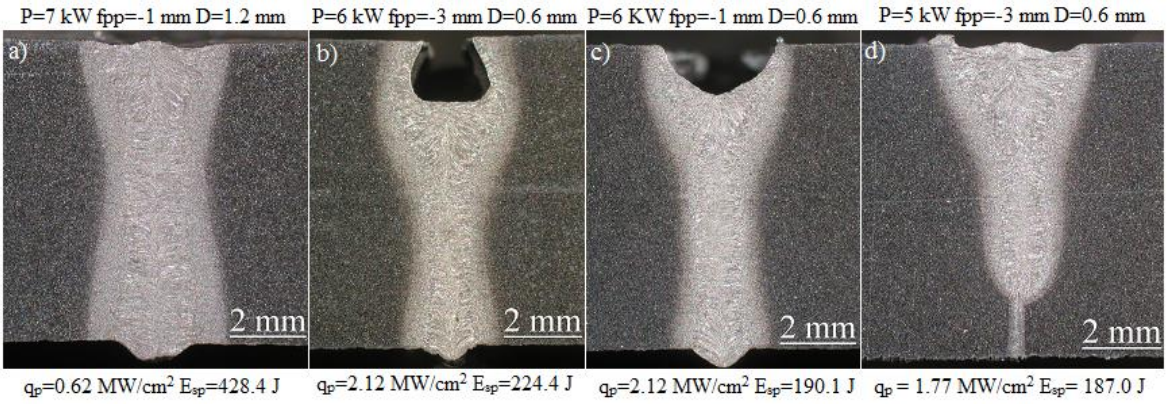

Figure 6. Effect of specific point energy and power density on penetration depth. Welds b) and c) are only partially full penetration, as seen from figure 7.

A closer look at the two partial penetration welds of figure 6 support the claim that a certain specific point energy is needed for a given power density to achieve complete penetration. From figure 7 can be seen the roots of the partial penetration welds done with the same power density of 2.12 MW/cm^2, but the specific point energy was increased from 190.1 J to 224.4 J by changing the focal point position from -1 mm to -3 mm. The welding process was unstable for the whole length of the weld with the specific point energy of 190.1 J. With increased specific point energy of 224.4 J, the process was also unstable at

first, but after the first half of the weld length, the process stabilized and a full penetration weld was produced for the latter part of the joint. This is most likely caused by the increased temperature of the base material during the welding process. At the end of the joint the temperature of the base material has risen, compared to the temperature at the beginning, which increases the absorption just enough for sufficient amount of energy to be transferred from the beam to the work piece, enabling complete penetration. The fact that this evolving into full penetration weld happened for only the weld with higher specific point energy to begin with, suggests that it was closer to the threshold value of specific point energy needed for full penetration at given power density of 2.12 MW/cm^2. Subsequently, the increase in absorption that happened along the weld length was sufficient to increase the energy that is transferred to the material just over the threshold value and a full penetration was achieved.

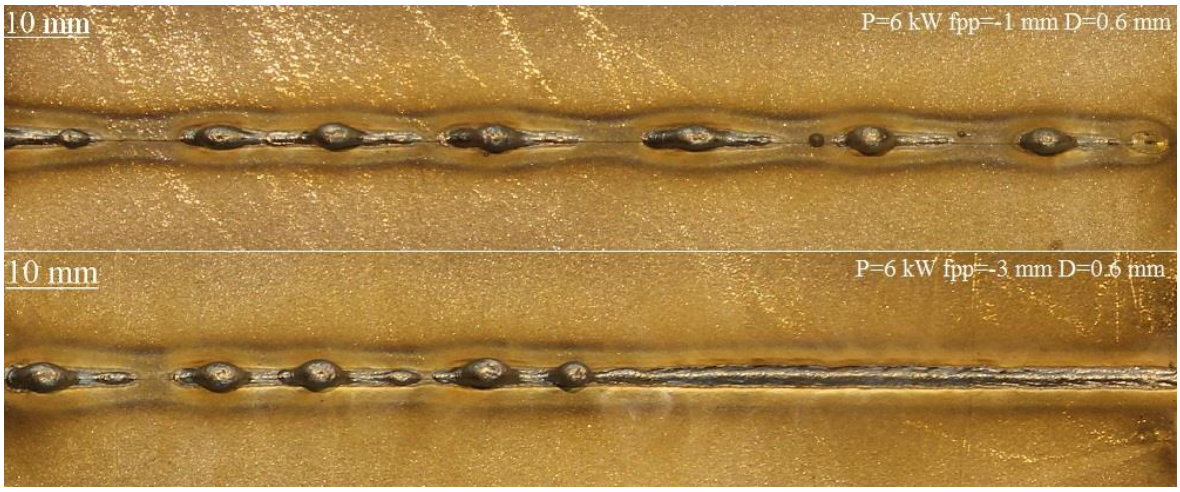

Figure 7. Root sides of the partial penetration welds.

4.2 Weld width

In addition to visual inspection of the macrographs, JMicroVision software was used to measure width, area and penetration of each weld cross-section seen from table 4. Width of the root isn't defined for welds with incomplete penetration. In case of welds 7 and 9, the process was unstable resulting in an incompletely filled groove and therefore the surface width can't be defined. The values for surface width in these two welds are estimates of what the width would be if the weld bead had formed properly. Some trends of the effect of parameters such as interaction time, point diameter at surface and specific point energy

on the weld width can be observed, but none of these alone can be used to predict the width of the produced weld, as explained below.

Table 4. Weld-bead geometry measured from macrographs.

Experiment	Width - surface [mm]	Width - middle [mm]	Width - root [mm]	Cross-sectional area [mm^2]	Penetration [mm] full = 8.0
1	2.3	0.9	1.1	8.5	full
2	3.3	1.2	1.9	13.4	full
3	2.6	1.1	1.4	10.8	full
4	3.3	1.2	2.0	13.2	full
5	3.2	1.4	2.2	15.5	full
6	2.9	1.7	2.0	15.6	full
7	3.4 (N/D)	1.0	1.6	9.4	partial
8	2.0	1.1	1.3	9.0	full
9	2.2 (N/D)	1.0	1.4	10.0	partial
10	3.6	1.6	(N/D)	12.8	7.0
11	1.9	1.1	1.0	8.4	full
12	2.8	1.3	(N/D)	8.9	6.0
13	3.5	0.9	(N/D)	9.6	6.3
14	2.9	1.5	(N/D)	10.2	6.0

As welding speed was kept constant in all experiments, beam diameter at surface is the only factor affecting the interaction time, based on equation 4. Figure 8 shows cross-sections of two welds done with constant beam diameter at surface (0.46 mm) and constant interaction time (21.98 ms). From the cross-sections it can be seen that constant interaction time and beam diameter at surface doesn't result in the same weld width, as it is increased when laser power is increased from 5 kW to 7 kW. Especially the surface width of the weld is increased, as the size of the melt pool at the surface of the material is increased with higher laser power.

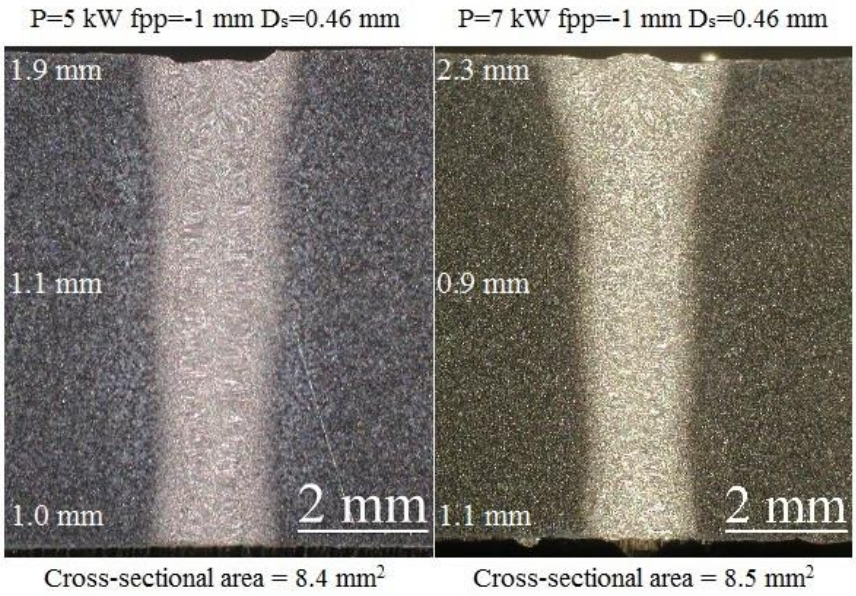

Figure 8. Effect of laser power on weld width, with constant interaction time and beam diameter at surface. Weld widths measured from the surface, middle and root can be seen on the left side of each weld.

The results suggests that interaction time alone can't be used to define the weld width, as it also depends on the laser power. This indicates that specific point energy could be the defining factor, as it considers both the interaction time and laser power, as equation 6 implies. As can be seen from figure 9, this is not the case. Increasing laser power or interaction time leads to an increase in the specific point energy. In other words, increase in specific point energy should cause an increase in the weld width. Figure 9 shows that when the specific point energy was increased from 221.8 J to 252.0 J, this resulted in a much narrower weld, opposed to the prediction that increasing specific point energy would increase the weld width. As laser power and welding speed were kept constant in both welds, the change in specific point energy was achieved by changing the focal point diameter on surface of the sample by varying focal point position and focal point diameter. The result indicates that these two parameters alone have an effect on the weld width, not interaction time or specific point energy, which both include the two aforementioned parameters.

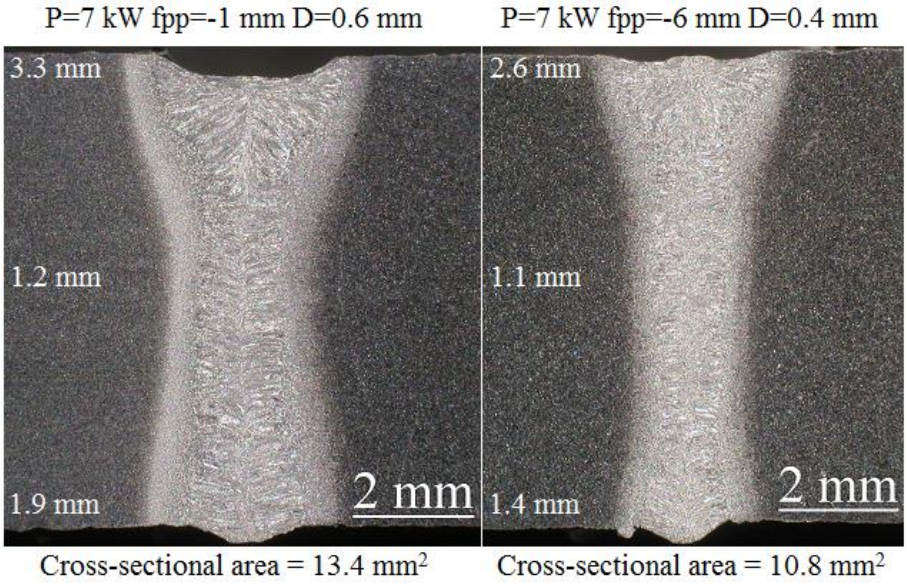

Figure 9. Weld width is not defined by the specific point energy. Increase in specific point energy from 221.8 J to 252.0 J produced a much narrower weld. Weld widths measured from the surface, middle and root can be seen on the left side of each weld.

The effect of focal point diameter on weld width was studied in an experiment with constant laser power of 7 kW and focal point position of -1 mm, but with three different transport fiber diameters of 200 µm, 300 µm and 600 µm, producing focal point diameters of 0.4 mm, 0.6 mm and 1.2 mm when focused on the surface of the specimen (0 mm), respectively. As the focal point position was -1 mm in all three experiments, the change in beam diameter at surface depends only on the transfer fiber used, resulting in values of 0.46 mm, 0.66 mm and 1.28 mm. From figure 10 it can be seen that size of the beam point diameter on surface is correlated with the width and cross-sectional areas of the welds. However, this does not explain whether the focal point diameter or the beam diameter at surface is responsible for the increase in weld width, as it can be also seen that as the focal point diameter increases, the weld width increases.

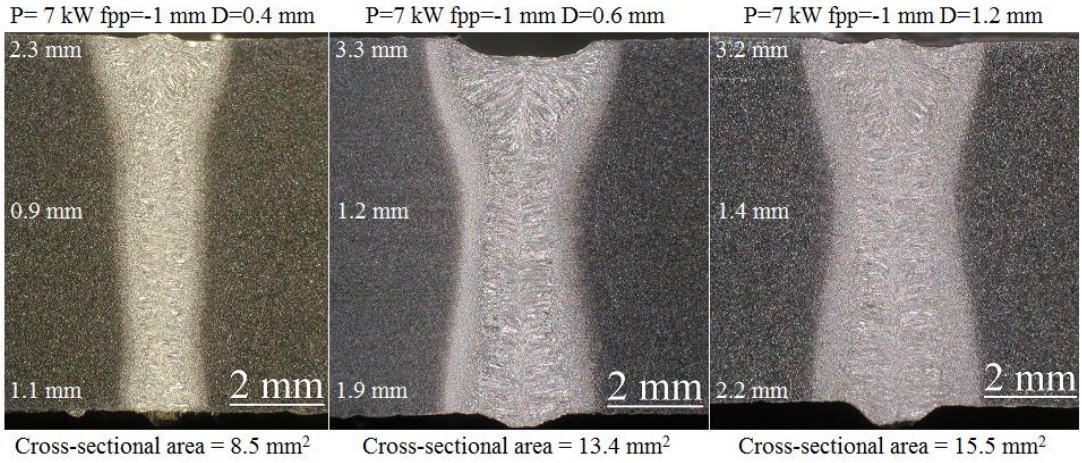

Figure 10. The effect of focal point diameter on weld width. The different focal point diameters were produced by varying the transfer fiber diameter. Weld widths measured from the surface, middle and root can be seen on the left side of each weld.

To find out whether the increase in weld width shown on figure 10 can be contributed to the increase in focal point diameter or to the increase in beam diameter at surface, two more welds produced using the same transfer fiber (200 µm, focal point diameter 0.4 mm) were compared. The beam diameter at surface was changed from 0.46 mm to 0.75 mm, by changing the focal point position from -1 mm to -6 mm, with constant laser power of 7 kW. As the beam diameter at surface increased and the focal point diameter remained constant, the weld width increased, as seen from figure 11. This would indicate that the weld width depends on the beam diameter at surface, not on the focal point diameter. To test this, a third experiment was done.

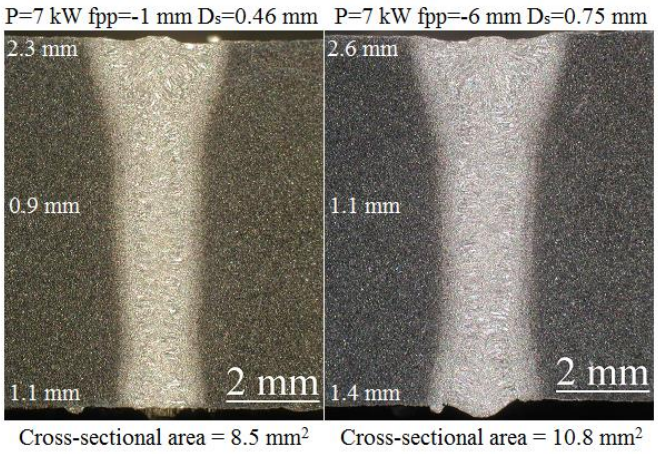

Figure 11. Effect of beam diameter at surface on weld width. Weld widths measured from the surface, middle and root can be seen on the left side of each weld.

Assuming that the weld width is controlled by the beam diameter at surface, when laser power and welding speed is kept constant, then changing focal point diameter and focal point position simultaneously to achieve same beam diameter at surface should result in welds with same width. In an experiment to test this, focal point diameter was changed from 0.4 mm to 0.6 mm by changing the transfer fiber from 200 µm to 300 µm and focal point position was changed from -6 mm to -3 mm, resulting in beam diameters at surface of 0.75 mm and 0.78 mm, respectively. Even if the beam diameters at surface are not exactly the same, the difference is only 4 % and should only result in extremely small changes in the weld width, as constant beam diameter at surface should yield welds with the same width, if the hypothesis is correct. However, figure 12 shows that there is a considerable difference in the weld width that cannot be explained by the 0.03 mm difference in the beam diameter at surface.

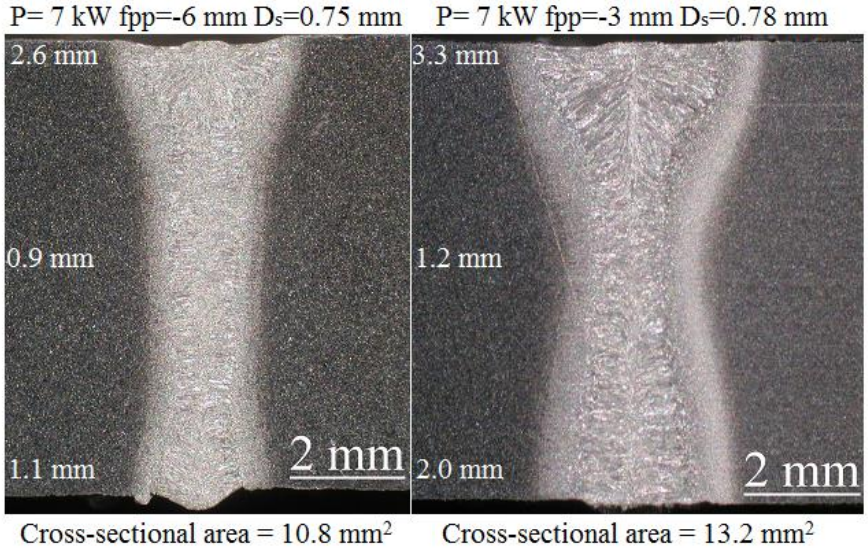

Figure 12. Weld width isn't defined by the beam diameter at surface, but rather by the focal point diameter and focal point position separately. Weld widths measured from the surface, middle and root can be seen on the left side of each weld.

This indicates that the weld width cannot be predicted with knowledge of beam diameter at surface alone, as welding speed and laser power are kept constant, but it is controlled individually by the focal point diameter and focal point position. Combining these two parameters into calculating beam diameter at surface and further, interaction time, seems to fail in defining the width of the weld produced. This could be explained by the geometry of the keyhole and the behavior of the melt pool around it. Beam diameter at surface considers

the focal point position only as a factor contributing to the size of it. However, as the focal point position is changed, the keyhole geometry changes, which ultimately controls the melt pool around it, and hence controls the weld width, as the molten material solidifies.

4.3 Mechanical properties

Base material hardness of around 140 HV5 was used as a reference point for the increase in hardness at the welded zone, measured from the middle of the weld cross-sections. The highest hardness values were measured from the fusion line as could be expected. First, the effect of focal point diameter on the maximum weld hardness was studied. As laser power and focal point position were kept constant, increasing the focal point diameter from 0.4 mm to 1.2 mm results in an increase in the maximum weld hardness from 301 HV5 to 381 HV, seen from figure 13. In the next experiment, laser power and focal point position were kept constant, to see the effect of focal point position on the weld hardness. As the focal point diameter changes from -1 mm to -3 mm, the maximum hardness is decreased from 379 HV5 to 343 HV5, seen from figure 14. In the third experiment, laser power was increased from 5 kW to 7 kW and focal point diameter and focal point position were kept constant, which results in a decrease in the maximum weld hardness from 343 HV5 to 320 HV5, seen from figure 15. To summarize, increasing the focal point diameter results in an increased weld hardness, increasing laser power results in decreased weld hardness and changing the focal point deeper below the surface of the material results in decreased weld hardness.

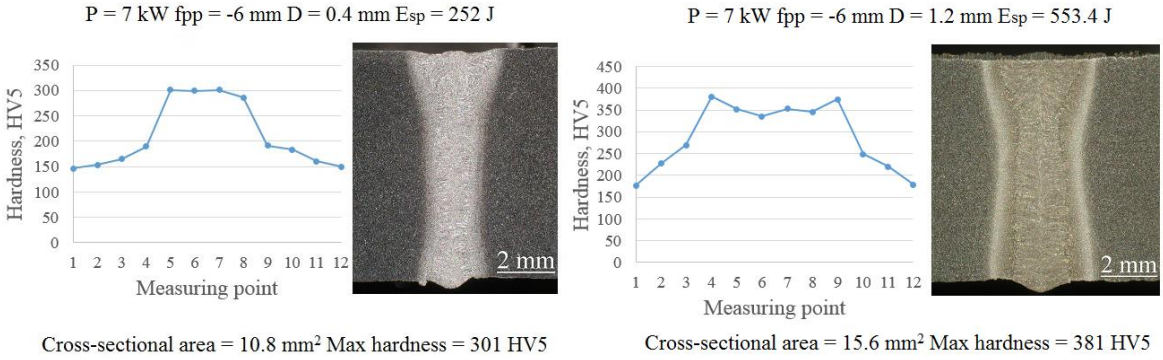

Figure 13. Effect of focal point diameter on weld hardness.

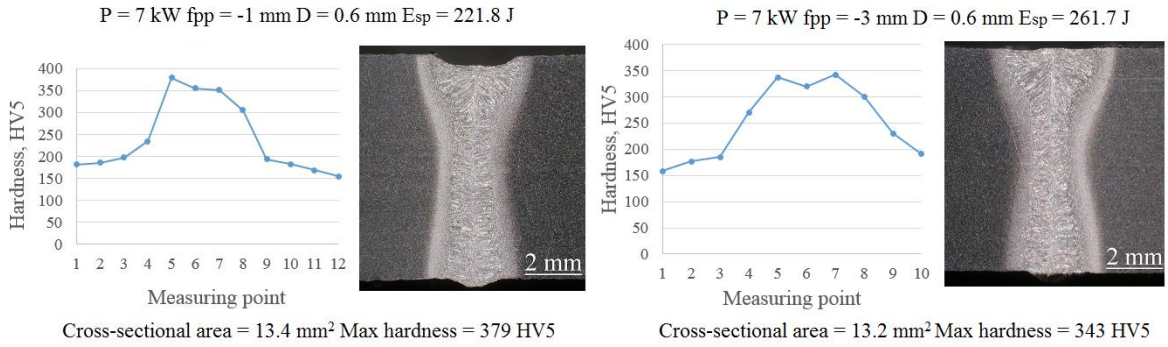

Figure 14. Effect of focal point position on weld hardness.

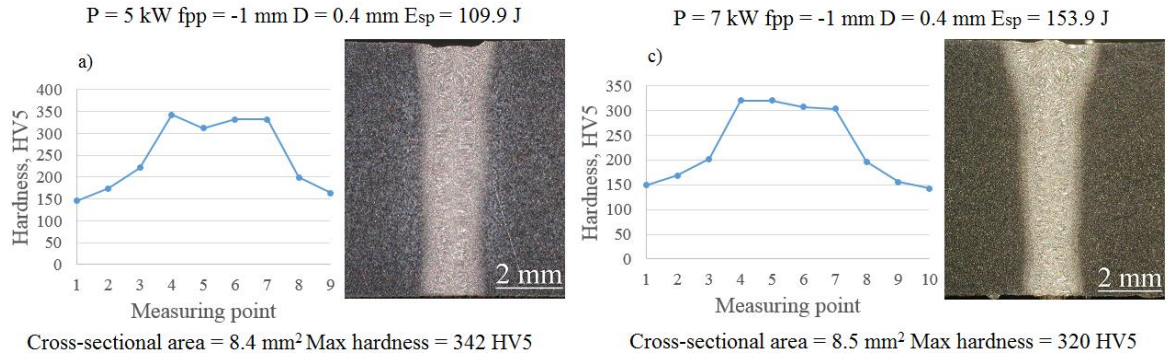

Figure 15. Effect of laser power on weld hardness.

In figure 15, as laser power is increased from 5 kW to 7 kW and all the other parameters are kept constant, the cross-sectional areas of the produced welds are almost the same, at 8.4 mm^2 and 8.5 mm^2 respectively. However, increasing the laser power increases the specific point energy from 109.9 J to 153.9 J, based on equation 6. This means that with 7 kW laser power, more energy is brought to the process, the cooling time is increased and as a results, the maximum weld hardness is reduced from 342 HV5 to 320 HV5. The same mechanism explains the difference in weld hardness seen in figure 14. As the focal point position is changed from -1 mm to -3 mm and all the other parameters kept constant, the specific point energy is increased from 221.8 J to 261.7 J. In this case also, the cross-sectional areas are almost the same, at 13.4 mm^2 and 13.2 mm^2, so the increase in the specific point energy causes the decrease in the maximum weld hardness from 379 HV5 to 343 HV5.

Figure 13 shows the effect of cross-sectional area on the weld hardness. As the focal point diameter is increased from 0.4 mm to 1.2 mm and all the other parameters kept constant,

the cross-sectional area increases from 10.8 mm^2 to 15.6 mm^2. Concurrently, increasing the focal point diameter increases the beam diameter at the surface of the material, which means that the specific point energy is also increased from 252.0 J to 553.4 J. The result is, that the maximum weld hardness is increased from 301 HV5 to 381 HV5. The increase in specific point energy should result in a decrease in the maximum weld hardness, but as the cross-sectional area is also increased, the effect of specific point energy is countered and furthermore, dominated by the effect of the cross-sectional area. This suggests that cross-sectional area of the weld has more drastic effect on the weld hardness, than specific point energy. In this case the specific point energy is increased by 119.6 % and the cross-sectional area by 44.4 % and still the hardness is increased, based on the increase in the area from which the heat conducts.

5 DISCUSSION

In this thesis the quality and hardness of the welds were evaluated according to EN ISO standards that are widely used in the industry and also in the scientific community, so that the results of this thesis can be used in comparison with other studies. The values used for focal point diameter in this thesis are theoretical values (see equation 2) and therefore the true values for power density, beam diameter at surface, interaction time and specific point energy slightly differ from those presented in this thesis. The actual value of the beam diameter at focal point can be measured with a beam analyzer, but the difference to the theoretical value is so small, that the use of theoretical values for the focal point diameter is justified.

Many authors have studied the laser keyhole welding process through the characteristics of the focal point. Power density, focal point diameter and focal point position all have an effect on the penetration depth and geometry of the welds produced. Suder & Williams (2012, p. 032009-1–032009-10) proposed that the process can be uniquely defined by three parameters: power density, interaction time and specific point energy. In this study, as in theirs, it was found that power density and specific point energy correspond well to the penetration depth that is achieved.

It is well known that the cooling rate of the molten material defines the hardness of the welded zone. Rapid cooling results in high hardness values at the weld metal and by slowing down the cooling rate, the increase in the weld hardness can be reduced. To understand the effects of focal point parameters on the weld hardness, the factors affecting to the cooling rate of the melt pool need to be considered. In laser welding, the cooling rate is defined by the energy that is brought to the process and by the area from which the heat conducts to the base material. Increasing the energy that is brought means that there is more heat that needs to be conducted away from the melt pool, hence it takes more time for the molten material to cool down. On the other hand, increasing the area from which the heat can conduct away, decreases the cooling time. In this study, specific point energy is used to define the energy brought to the process and cross-sectional area of the weld is used to evaluate the area, from which the heat conducts.

The results of this thesis suggest that specific point energy is more accurate definition for the energy that is brought to the process than line energy, which is typically used in evaluating the weld hardness. If we look at figure 14 and calculate line energies for the welds, both of them have the same value of 336 J/mm for the line energy, because the laser power and welding speed are kept constant. Also the cross-sectional areas are almost the same for both, at 13.4 mm^2 and 13.2 mm^2. Since the cooling rate is depended on the energy that is brought to the process and on the area from witch it conducts away, these two welds should have the same hardness values based on the line energy. As seen from figure 14, this is not the case, as the maximum weld hardness is decreased from 379 HV5 to 343 HV5, a difference of roughly 10 %. This can be explained with the specific point energy, which is different for these welds, at 221.8 J and 261.7 J, as opposed to the line energy that doesn't consider the point diameter and hence is the same. The difference in the specific point energy explains the difference in the resulting weld hardness, as the higher specific point energy reduces the cooling rate, which in turn reduces the weld hardness.

The specific point energy introduced by Suder & Williams (2012, p. 032009-1–032009-10) seem to work well in defining the penetration depth and weld hardness in the process of fiber laser keyhole welding, but the same study also suggested that weld width is dependent on the interaction time and independent of the beam diameter. Increase in the interaction time should lead to an increase in the weld width (Suder & Williams, 2012, p. 032009-6). The results of the experiments done in this thesis however contradict with this claim. It is shown that with constant interaction time, increasing the laser power increases the width of the weld produced. Also wider welds can be produced even if the interaction time is decreased, as can be seen from figure 9. In the experiment the weld produced with interaction time of 36.00 ms resulted in a much narrower weld than the one produced with shorter interaction time of 31.68 ms. Based on these findings it seems that interaction time alone can't be used to define the weld width.

Humping is observed in the welds with high power densities. The same phenomena has been described by Katayama et al. (2010, p. 9–17). Humping can be avoided by decreasing the power density and increasing specific point energy instead to achieve the desired depth of penetration. In practice this means increasing the focal point diameter, as reducing the laser power would also reduce the specific point energy and would reduce the penetration

depth. Increasing the focal point diameter will increase the specific point energy, but simultaneously it will reduce the power density. However, as long as the power density is sufficient, full penetration can be achieved and the humping eliminated.

Cross-sectional area of the weld is used in this thesis as a measure for the area, from which the heat conducts to the base material from the melt pool. In reality, the area, from which the heat is conducted, is the surface area around the keyhole. Defining this area requires 3D modelling of the keyhole and this needs to be done individually for all the welds, as the keyhole geometry is different with different parameters. 3D construction of the keyhole requires in-situ X-ray videography or high-speed videography of the welding process, to obtain images of the keyhole geometry. Measuring the cross-sectional areas is much easier and less time consuming and these values can be used to explain the differences in cooling times, as increase or decrease in the cross-sectional area also leads to the increase or decrease of the surface area around the keyhole respectively, which ultimately defines the cooling rate, together with the energy brought to the process.

6 CONCLUSIONS

Based on the literature review and the welding experiments done, the following conclusions could be drawn:

1. The penetration depth depends mainly on the power density and specific point energy.
2. Width of the weld is not defined by the interaction time.
3. Weld hardness is controlled by the cooling rate, which in turn depends on the energy brought to the process and on the area from which the heat conducts to the base material.

Increase in power density or specific point energy increases the penetration depth. For the fundamental process parameters in laser welding, this means that increase in laser power always increases the penetration depth, as increase in laser power increases both power density and specific point energy, as seen from equations 3 and 6. If the power density is increased by decreasing the focal point diameter, simultaneously the specific point energy is reduced. However, as seen from equations 3 and 6, decrease in the focal point diameter leads to an exponential increase in the power density and the specific point energy only decreases linearly, hence the penetration depth is still increased. Changing the focal point position deeper below the surface of the material increases the beam diameter at the surface of the material, increasing specific point energy and hence the penetration depth is increased. Concurrently, the increase in beam diameter at surface reduces the power density at the surface of the material and the penetration depths starts to decrease when the focal point position is placed too deep inside the material.

Width of the weld is defined by the geometry of the melt pool, which in turn is controlled by the keyhole geometry and laser power. Geometry of the keyhole is affected by many parameters, such as welding speed, laser power, focal point position and focal point diameter. This makes it a complicated task to predict the weld width, as it was show in this thesis that combining these process parameters to form parameters such as interaction time and specific point energy and trying to explain the changes in weld width with these two parameters, doesn’t work. Based on the welding experiments, increasing laser power increas-

es the weld width, especially on the surface of the weld and increasing focal point diameter with constant focal point position, also increases the weld width. However, it seems that changes in the focal point position between -1 mm, -3 mm and -6 mm doesn't have any linear relation with weld width, but it is clear that it has an effect on the weld width. Change in the focal point position has an effect on the geometry of the keyhole and therefore on the weld width. Based on the findings, it seems that the studies on understanding the formation of the weld width should be conducted through the studies of the keyhole geometry and melt pool behavior.

Increase in the hardness of the weld metal is undesirable, but it can be controlled with the parameters of the focal point. Decreasing the area, from which the heat conducts, results in decreased weld hardness. The most effective way to decrease the area, is achieved by decreasing the focal point diameter. The other way to control the weld hardness is to change the energy that is brought to the process, as more energy results in decreased weld hardness. This is achieved either by reducing the laser power, increasing the focal point diameter or placing the focal point position deeper below the surface of the material. However, change in the process parameters simultaneously affects both the energy and area, so finding the right combination of parameters to achieve minimal increase in the weld hardness without losing full penetration, requires good understanding of the process.

Full penetration welds can be achieved even if the focal point diameter is increased in order to achieve a wider weld to ease the gap tolerances set for laser welding, as long as the increase in specific point energy is high enough to counter the decrease in power density. In this study, B quality welds were achieved with all focal point diameters of 0.4 mm, 0.6 mm and 1.2 mm, but it should be noted that the weld hardness increased as the focal point diameter increased. This indicates that if a wider weld is produced to ease the gap tolerances, mechanical properties of the joint may be reduced and this needs to be considered, depending on the application of the joint.

6.1 Further studies

The hardness tests showed that there are considerable differences in the increase of hardness's between welds performed with different combinations of laser power, focal point position and focal point diameter. Increase in weld zone hardness only indicates that the

mechanical properties of the joint have changed. To have a comprehensive view of how the parameters of the focal point affect the mechanical properties of the joint, fracture toughness, tensile properties and flexural properties should be tested.

It was also suggested, that in case of laser welding, specific point energy could be more accurate definition for the energy brought to the process than line energy. Line energy doesn't consider the diameter of the laser beam as a contributing factor to the amount of energy that is brought to the process. Therefore, in the experiments of this study, line energy fails to explain differences in hardness values between welds with same cross-sectional areas, whereas specific point energy succeeds in this. This was only noted during the analysis of the results and therefore is not studied in depth on this thesis. The hypothesis that specific point energy is more accurate than line energy in evaluation of weld hardness in laser keyhole welding should be studied in more detail.

7 SUMMARY

Laser keyhole welding is a viable process for the welding industry, as it offers considerable lower heat input than arc welding processes and therefore distortions in the product are kept in minimum. In laser welding, the power density is high enough to generate a keyhole, which enables deep penetration in a single pass, making it a competitive process against multi-pass arc welding. In this thesis, the effect of focal point parameters in fiber laser welding of structural steel was studied. The goal was to find out how focal point diameter, focal point position and laser power brought to the focal point affects the quality, geometry and hardness of the welds produced. Previous studies relating to the topic were researched and a background was established.

A set of welding experiments were done on AH36 structural shipbuilding steel to see the effects of changing focal point diameter, focal point position and laser power. Visual inspection of the weld surface, root and cross-sections was done to evaluate the quality and geometry of the welds produced and Vickers hardness test was used to measure the hardness of the welds produced. The results of the welding experiments were compared with the results found out by other authors in previous studies. Especially it was of keen interest to find out whether the equations introduced by Suder & Williams (2012, p. 032009-1–032009-10) for interaction time and specific point energy can be used in defining the penetration depth, width and hardness of the welds produced.

The quality of the welds were analyzed based on standard SFS-EN ISO 13919-1 (1996) and in the welds produced, incomplete penetration was the only imperfection leading to an unacceptable weld. Humping was observed in welds produced with high power densities and spatters were generated in some welds, but these imperfections were not severe enough to lower these welds from the highest quality level B, which is defined in the standard. It was found that incomplete penetration is caused by insufficient power density or insufficient specific point energy. Increasing power density or specific point energy increases penetration depth.

The effect of focal point parameters on the weld geometry was studied by measuring the widths and cross-sectional areas of the welds from the macrographs of the weld cross-sections. It was found that the geometry of the weld is depended on various parameters, such as laser power, welding speed, focal point position and focal point diameter. These process parameters affect the weld width through the geometry of the keyhole, which depends on the process parameters.

Vickers hardness's measured from the middle of the cross-sections of the welds showed that the focal point parameters affect the weld hardness through the energy that is brought to the process and the area, from which the heat conducts to the base material from the weld zone. In this thesis, specific point energy was used to define the energy that is brought to the process and it was shown that increase in the specific point energy results in a decrease in the weld hardness. Cross-sectional area of the weld was used a measure to define the area, from which the heat conducts and it was shown that increase in the area results in an increase in the weld hardness.

REFERENCES

Brown, C. O. & Banas, C. M. 1971. Deep penetration laser welding. American Welding Society 52nd Annual Meeting. 26–29 April 1971. San Francisco, CA, USA.

Cleemann, L. 1987. Schweissen mit CO2-Hochleistungslasern. Düsseldorf, Germany: VDI-Verlag GmbH. Technologie Aktuell 4. 256 p.

Dausinger, F. & Weberpals, J. 2007. Influence of inclination angle on spatter behavior at welding with lasers of strong focusability. Congress proceedings. ICALEO 26th International Congress on Applications of Lasers & Electro-Optics. October 29 – November 1 2007. Orlando, FL, USA. Laser Institute of America. P. 858–865.

Einstein, A. 1916. Strahlungs-Emission und Absorption nach der Quantentheorie. Verhandlungen der Deutschen Physikalischen Gesellschaft. Volume 18. P. 318–323.

Einstein, A. 1917. Quantentheorie der Strahlung. Physikalische Zeitschrift. Volume 18. P. 121–128.

Hill, P. 2002. Fiber laser hits 2 kW record mark. Opto and Laser Europe (OLE). July/August 2002. P. 9.

International Institute of Welding. 1967. Technical Report. Doc. IX-535-67.

Ion, J. C. 2005. Laser Processing of Engineering Materials: Principles, procedure and industrial applications. Oxford: Elsevier Butterworth-Heinemann. 556 p.

IPG Photonics. 2015. Products - YLS Series. [Web document]. Updated 4.5.2015. [Referred 4.5.2015]. Available: http://www.ipgphotonics.com/apps_materials_multi_yls.htm

Katayama, S. 2013. Handbook of Laser Welding Technologies. Cambridge, UK: Woodhead Publishing. Elsevier. 654 p.

Katayama, S., Kawahito, Y. & Mizutani, M. 2010. Elucidation of laser welding phenomena and factros affecting weld penetration and welding defects. Physics Procedia. Volume 5. P. 9–17.

Kawahito, Y., Mizutani, M. & Katayama, S. 2007. Investigation of High-Power Fiber Laser Welding Phenomena of Stainless Steel. Transactions of JWRI. Volume 36. Issue 2. P. 11–15.

Kujanpää, V., Salminen, A. & Vihinen, J. 2005. Lasertyöstö. Tampere, Finland: Teknologiainfo Teknova Oy. 373 p.

Maiman, T. 1960. Stimulated Optical Radiation in Ruby. Nature. Volume 187. P. 493–494.

Pastor, M., Zhao, H. & Debroy, T. 2001. Pore formation during continuous wave Nd:YAG laser welding of aluminium for automotive applications. Welding International. Volume 15. Issue 4. P. 275–281.

Quintino, L., Costa, A., Miranda, R., Yapp, D., Kumar, V. & Kong, C. J. 2007. Welding with high power fiber lasers – A preliminary study. Materials & Design. Volume 28, Issue 4. P. 1231–1237.

Ream, S. 2004. Laser welding efficiency and cost – CO_2, YAG, Fiber and disk lasers. Congress proceedings. ICALEO 23rd International Congress on Applications of Lasers and Electro-Optics. 4-7 October 2004. San Francisco, CA, USA. Laser institute of America. 5 p.

Salminen, A., Lappalainen, E. & Purtonen, T. 2013. Basic phenomena in high power fiber laser welding of thick section materials. 37th Matador Conference. CIRP, Manchester. 25-27 July 2012. Springer-Verlag London. P. 331–336.

Schawlow, A. & Townes, C. 1958. Infrared and Optical Masers. Physical Review. Volume 112. P. 1940–1949

SFS-EN ISO 6507-1. 2006. Metallic materials. Vickers hardness test. Part 1: Test method. Finnish Standards Association SFS. Helsinki, Finland. 22 p.

SFS-EN ISO 13919-1. 1996. Welding. Electron and laser beam welded joints. Guidance on quality levels for imperfections. Part 1: Steel. Finnish Standards Association SFS. Helsinki, Finland. 16 p.

SFS-EN ISO 17639. 2013. Destructive tests on welds in metallic materials. Macroscopic and microscopic examination of welds. Finnish Standards Association SFS. Helsinki. Finland. 13 p.

Steen, W. & Mazumder, J. 2010. Laser material processing. 4 edition. London: Springer London. 558 p.

Suder, W. J. & Williams, S. 2012. Investigation of the effects of basic laser material interaction parameters in laser welding. Journal of Laser Applications. Volume 24. Issue 3. P. 032009-1–032009-10.

Suder, W. J. & Williams, S. 2014. Power factor model for selection of welding parameters in CW laser welding. Optics & Laser Technology. Volume 56. P. 223–229.

Tenner, F., Brock, C., Klämpfl, F. & Schmidt, M. 2015. Analysis of the correlation between plasma plume and keyhole behavior in laser metal welding for the modelling of the keyhole geometry. Optics and Lasers in Engineering. Volume 64. P. 32–41.

Vänskä, M., Abt, F., Weber, R., Salminen, A. & Graf, T. 2013. Effects of welding parameters onto keyhole geometry for partial penetration laser welding. Physics Procedia. Volume 41. P. 199–208.

Xiangzhong, J., Yuanyong, C., Licheng, Z., Yufeng, Z. & Honggui, Z. 2012. Multiple Reflections and Fresnel Absorption of Gaussian Laser Beam in an Actual 3D Keyhole during Deep-Penetration Laser Welding. International Journal of Optics. Volume 2012. 8 p.

Photographs and macrographs of the welding experiments.

Top side (F), root side (R) and cross-section of the weld	Experiment
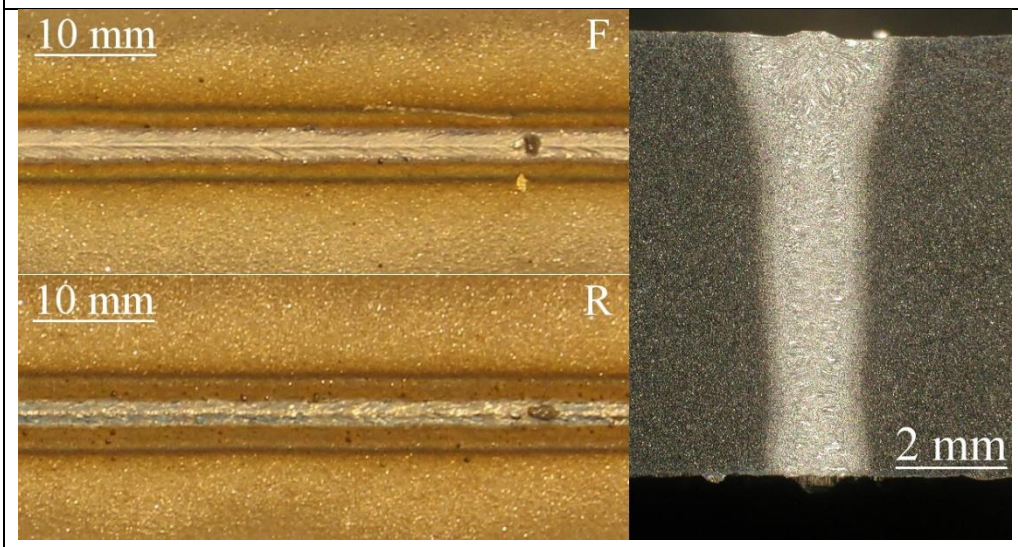	1
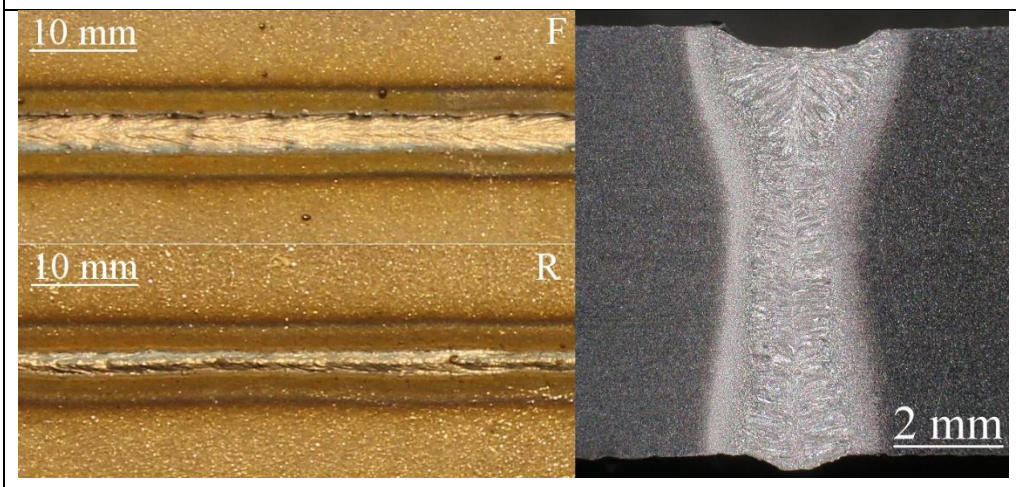	2
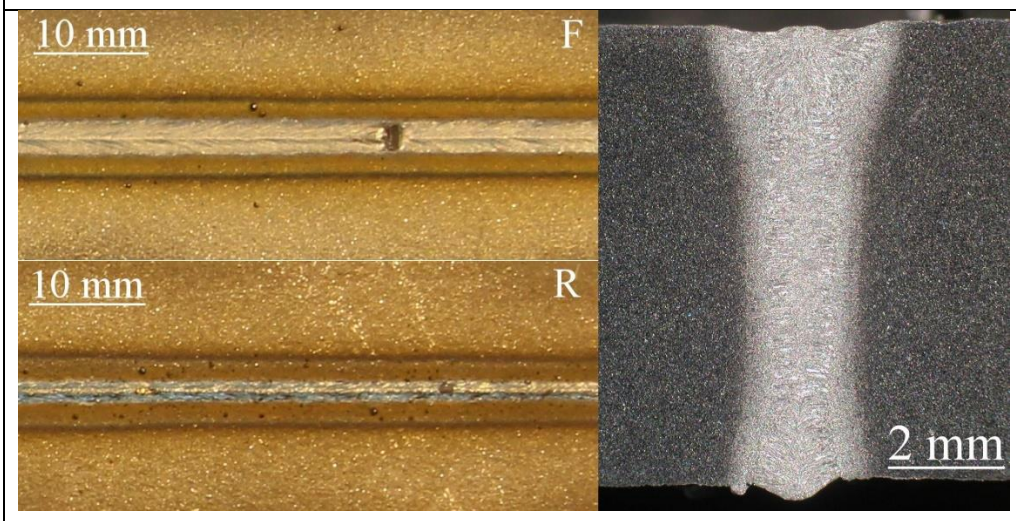	3

Top side (F), root side (R) and cross-section of the weld	Experiment
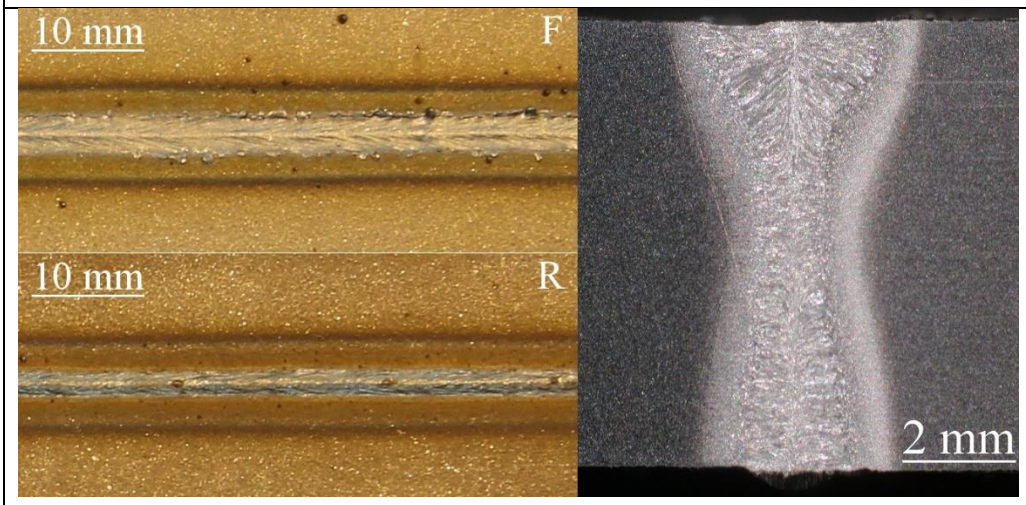	4
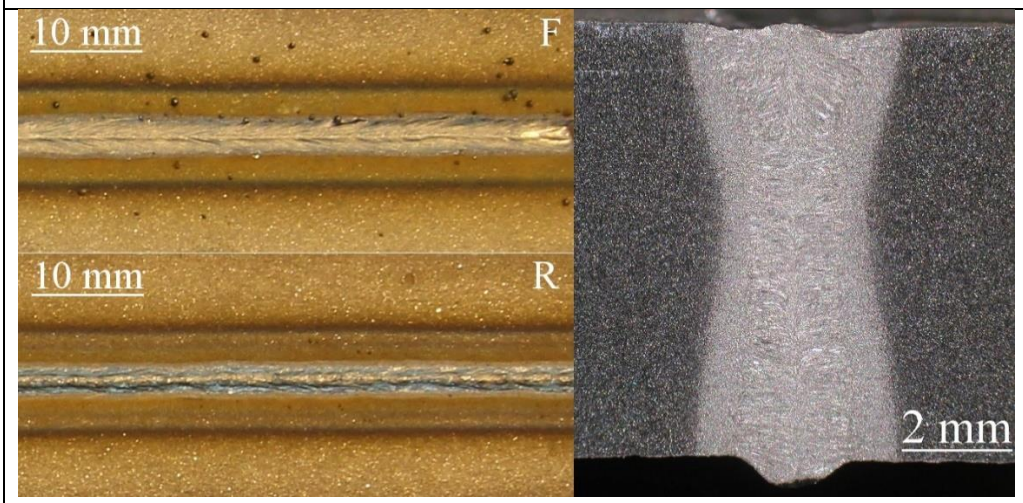	5
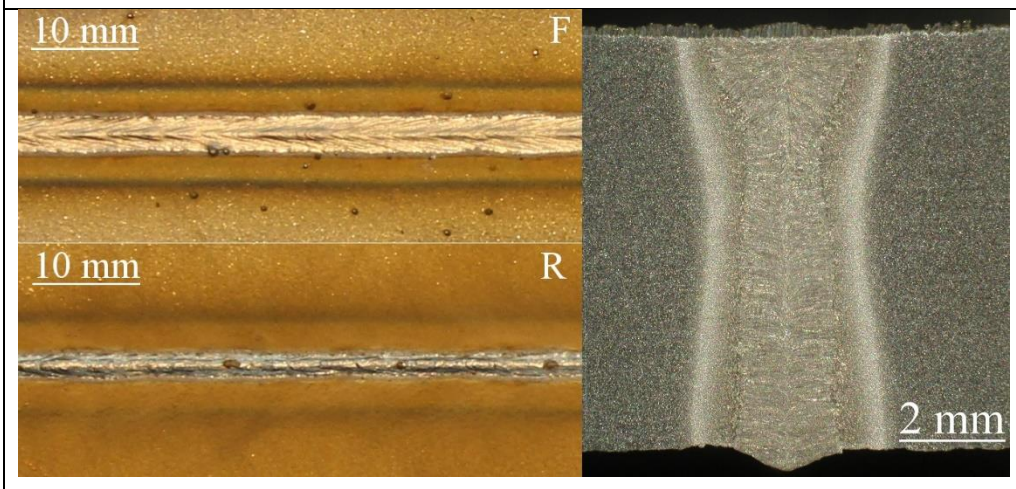	6

Top side (F), root side (R) and cross-section of the weld	Experiment
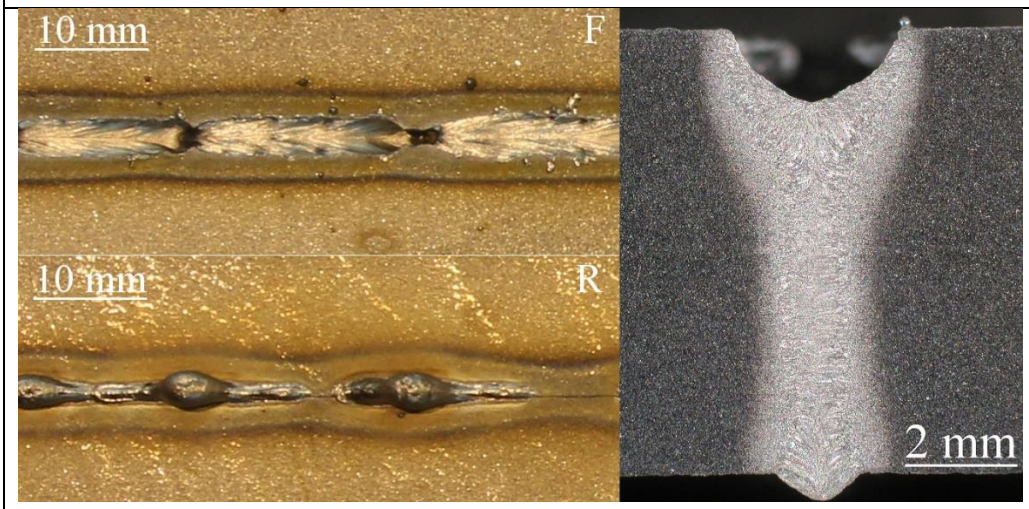	7
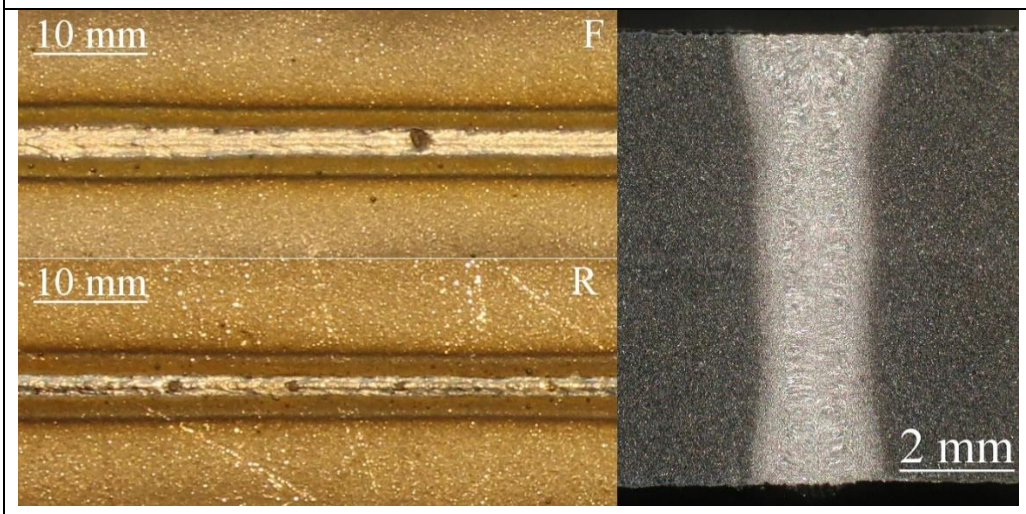	8
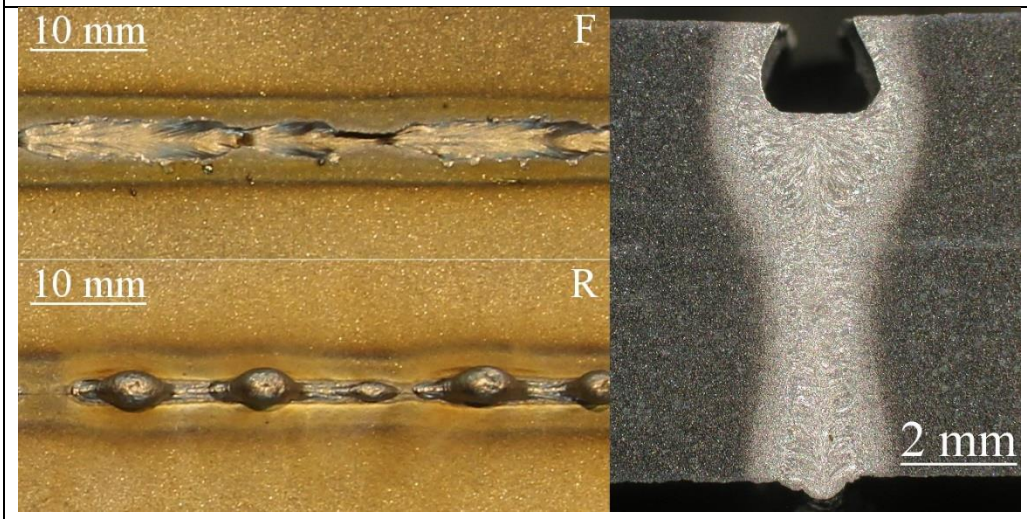	9

Top side (F), root side (R) and cross-section of the weld	Experiment
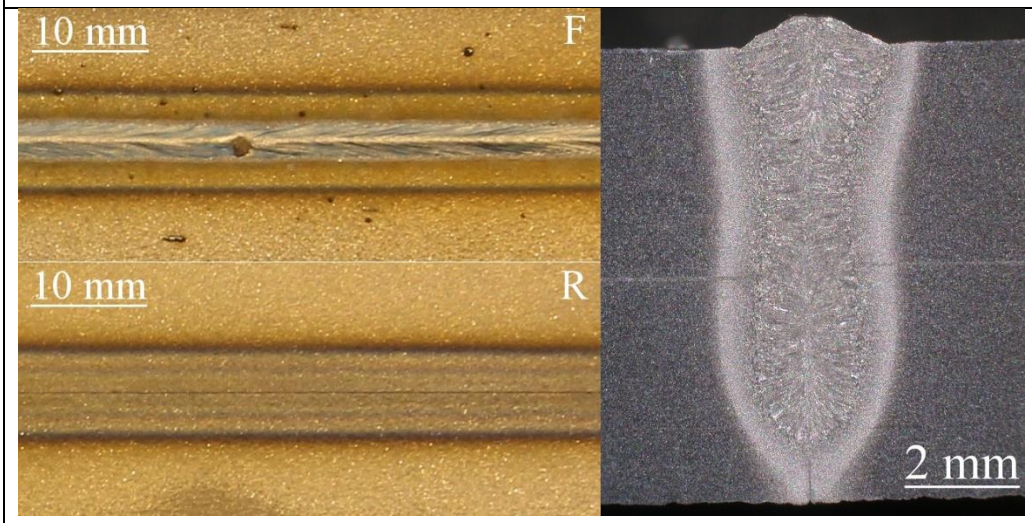	10
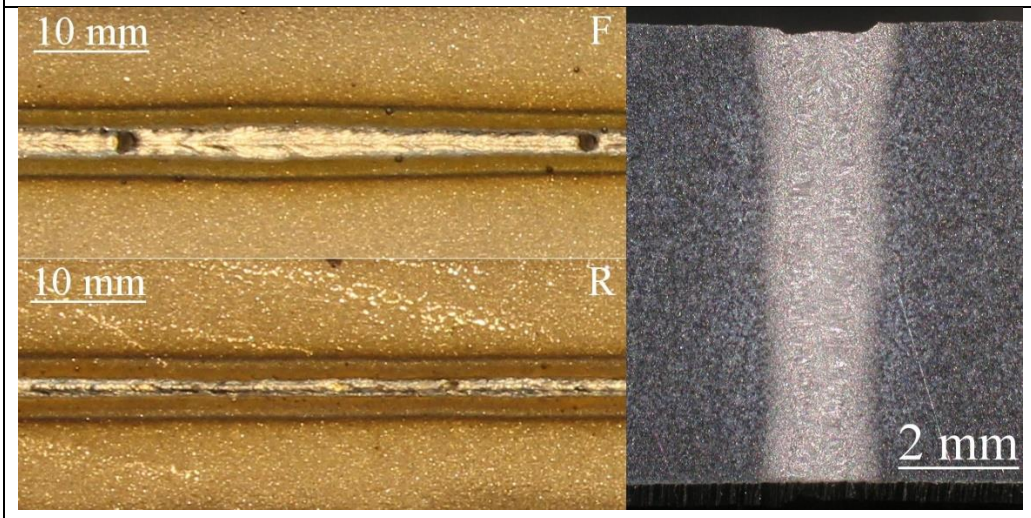	11
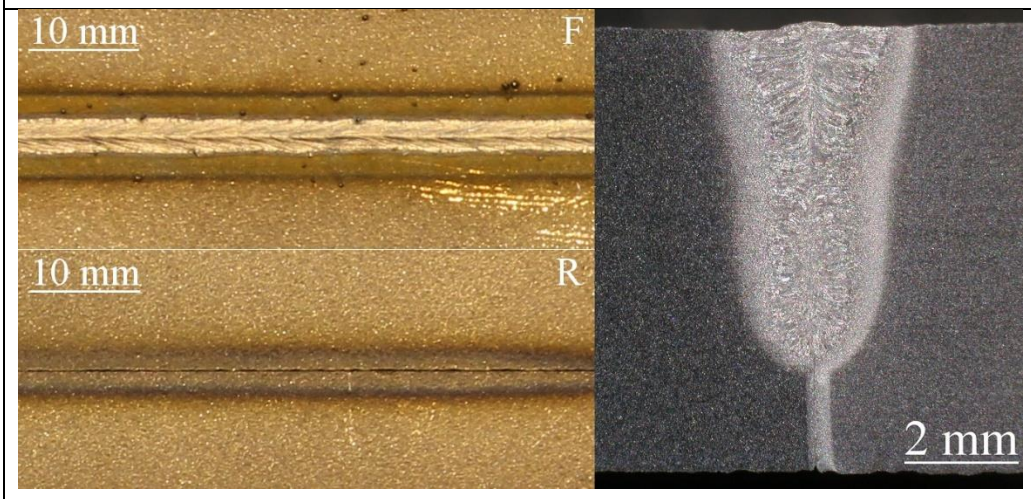	12

Top side (F), root side (R) and cross-section of the weld	Experiment
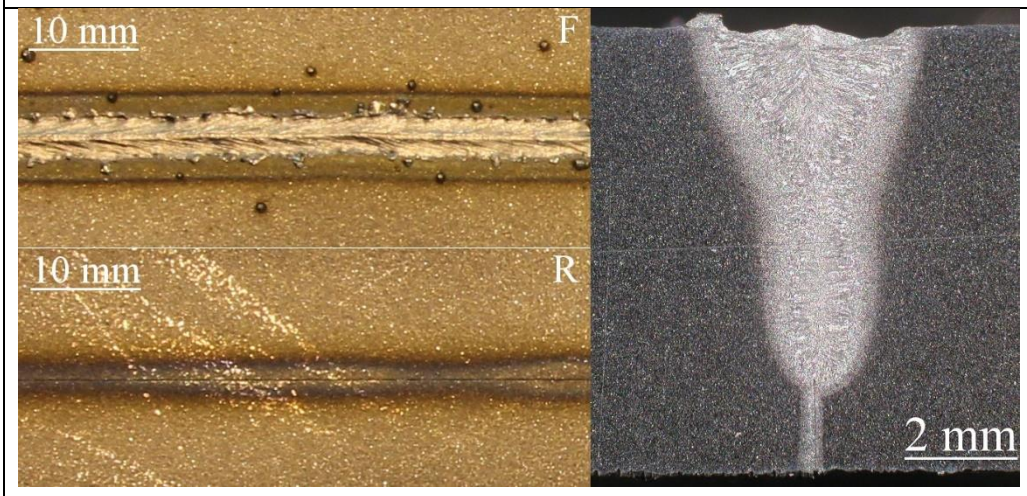	13
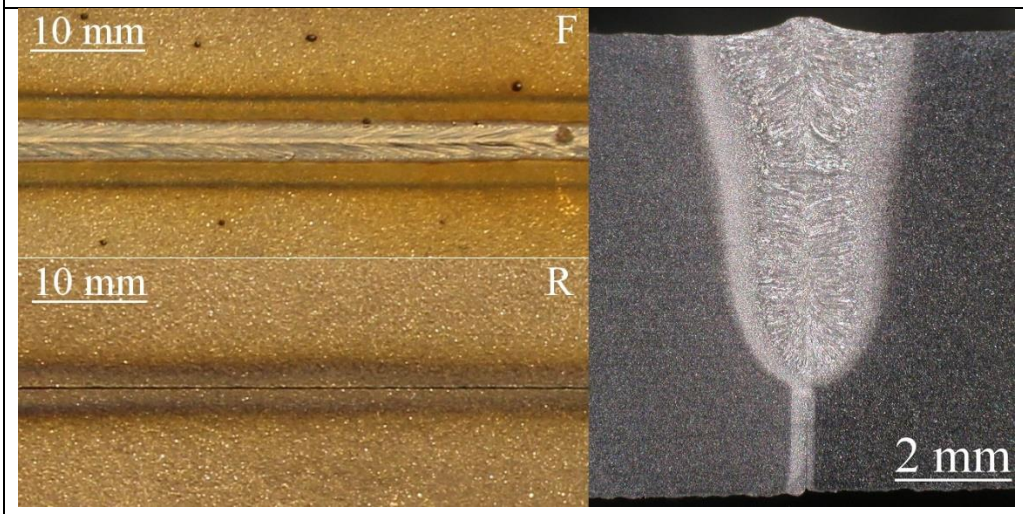	14